



# THE CONNECTIONS BETWEEN THE EVOLUTION OF VEGETATION COVER IN THE SOUTHERN ARAL SEA REGION AND THE TRANSPORT OF SALTS FROM THE DESICCATED SEABED OF THE ARAL SEA

Tleumuratova B. S.<sup>1</sup>,

Kublanov Zh. Zh.<sup>1,2</sup>,

Urumbaev A. E.<sup>1</sup>,

Nurmukhamedov I. I. <sup>1</sup>

<sup>1</sup>Karakalpak Research Institute of Natural Sciences,  
Karakalpak Branch of the Academy of Sciences of the Republic of Uzbekistan

<sup>2</sup>Center for Pedagogical Excellence of the Republic of Karakalpakstan

E-mail: [kublanov90@list.ru](mailto:kublanov90@list.ru),

[tbibigul@mail.ru](mailto:tbibigul@mail.ru),

[ametov.islam1369@gmail.com](mailto:ametov.islam1369@gmail.com)

## Abstract

This article examines quantitative changes in the vegetation cover of the Southern Aral Sea region as a whole, caused by the long-term impact (1961–2024) of salt transport from the dried-up Aral Sea bed. Excluding species transformations, the evolution of vegetation cover is considered here in terms of the reduction in areas covered by vegetation. Using modeling methods, the study aggregates the spatio-temporal dynamics of the total projected vegetation cover in relation to the average annual sulfate deposition from the Aralkum Desert. The research results are presented as formalized patterns of vegetation degradation and as cartographic representations of salt deposition fields from the dried seabed and the corresponding changes in total projected cover by decades from 1961 to 2024. The impact of salt transport is determined by dust deposition on plant root zones and by increasing soil salinity.

**Keywords:** Aral Sea region; salt transport; vegetation dynamics; aeolian processes; salinization; desertification; ecological succession; environmental degradation.

## Introduction

The Earth's vegetation cover (VC) is a fundamental component of the global biota, the significance of which can hardly be overestimated. The positive impact of vegetation on the environment is well known and determined by a wide range of ecosystem services. However, it is equally well known how enormous the damage caused to vegetation by human activities is. Ruthless deforestation, overgrazing, urbanization, and other factors contribute to a persistent trend of vegetation degradation in many regions of the planet.





In addition to anthropogenic stress, vegetation is currently experiencing climatic stress associated with more frequent droughts, extraordinary floods, and hurricanes due to global warming. Recognizing the major role of vegetation in climate regulation, dust and sand stabilization, and other environmental processes, numerous restoration efforts have been initiated worldwide. Among them, Norway's contribution to the restoration of the Amazon rainforest and China's creation of the "Green Wall" covering 100 million hectares are particularly noteworthy [14]. Nevertheless, even such large-scale measures do not reduce the global rate of vegetation degradation.

The degradation of vegetation cover is particularly dynamic in the Southern Aral Sea region—the epicenter of the Aral Sea crisis. Landscape evolution here tends toward the formation of desert complexes [4]. The deterioration of the hydro-saline regime has led to a sharp transformation of the floristic diversity of the region. For instance, reed-covered areas have decreased from 600 thousand hectares to 30 thousand hectares, while tugai forests have shrunk from 1,300 to 50 thousand hectares [17].

Salinization of deeper soil horizons worsens the edaphic conditions for typical xerophytes, leading to a gradual shift in species composition—from xerophytic to haloxerophytic and halophytic species. This transformation is accompanied by a general decline in vegetation density and the die-off of species that stabilize dune sands. On the Ustyurt Plateau, characterized by highly saline soils, additional chloride–sulfate salt input has particularly adverse effects on black saxaul (*Haloxylon aphyllum*), such as in the Assake-Audan depression [1].

The main drivers of floral changes in the Aral Sea region are the deterioration of the hydro-saline regime, decreased air humidity, increased vegetation-period temperatures, reduced precipitation, and the aeolian (wind-driven) transport of mineral aerosols from desert surfaces. The effects of all these factors, except the last one, have been relatively well studied by qualitative methods. To fill this gap, we have conducted studies on the impact of salt transport from the dried-up Aral Sea bed (DASB) on vegetation [9].

Mineral dust affects plants in two main ways: mechanically (by damaging stems, leaves, and flowers, depositing particles on leaves, and clogging stomata) and physiologically (by introducing pollutants into the rhizosphere through precipitation and their subsequent accumulation in plant tissues). The primary phytotoxic effect of salt dust manifests through disrupted respiration and photosynthesis processes, leading to the suppression of vegetative organs, necrosis, chlorosis, and leaf dieback. It has been reported that due to salt transport from the dried-up Aral Sea, cotton yield decreases by up to 10%, and pasture productivity drops by up to 50%. Currently, an average of 250 kg/ha of salts is deposited during each growing season. Furthermore, the accumulation of toxic sulfates in agricultural plants poses ecological safety risks when consumed as food [2].

Despite the environmental significance of aerosol pollution (both anthropogenic and natural), studies on its impact on vegetation remain limited. Moreover, the factor of atmospheric aerosol contamination is almost never considered as a criterion in optimizing agricultural land use, even though it should be ranked alongside key optimization parameters such as economic costs, natural resources, and climatic conditions.

For the Southern Aral Sea region, given the ongoing transport of salts from the dried-up Aral Sea bed, it is particularly relevant to delineate zones with varying levels of chloride–sulfate aerosol deposition. This is essential for selecting agricultural areas based on the criterion of minimizing



ecological stress from aerosol pollution.

The degree of air pollution is typically assessed using MAC (Maximum Allowable Concentrations) and TSEL (Tentatively Safe Exposure Levels). Based on these indicators ( $\text{mg}/\text{m}^3$ ), the environmental hazard class of pollutants is determined: for example, dioxins belong to Class I, while dust is assigned to Class III. However, none of these indicators have been defined for evaluating the effects of salt transport from the dried Aral Sea bed on plants. Therefore, we have initiated experimental studies to determine the degree of sodium sulfate (the dominant fraction of salt aerosols from the Aralkum) impact on plants [9].

According to the well-known thesis that “science is the search for regularities,” beyond isolated episodic manifestations of the studied process, it is of great scientific value to generalize and identify underlying trends and patterns. Therefore, the purpose of this study is to investigate the long-term dynamics of the impact of salt transport from the Aralkum on vegetation cover.

It should be noted that this study does not account for the bimodality of dry atmospheric deposition observed during severe salt-dust storms (SDS) due to their exceptional nature, even though the second mode (at a distance of 300–500 km) can be comparable in magnitude to the first, proximal one.

## Methods

In conditions of limited observational data, the most appropriate approach to studying the evolution of vegetation cover is the use of modeling methods in combination with remote sensing (RS) techniques. The study also employs statistical analysis and GIS technologies.

The calculations were carried out under the following assumptions and conditions: The dynamics of total projected cover (TPC) and salt transport from the Aralkum were averaged by decades over the study period (1961–2024) to eliminate interannual noise. Due to the extreme scarcity of ground monitoring data on TPC, it was assumed to be proportional to plant biodiversity (i.e., the number of species), for which more representative data are available.

The modeling domain encompasses the entire dried-up Aral Sea bed and adjacent territories extending up to 300 km along the normal to the 1961 shoreline (Fig. 1).



Figure 1. Modeling area.





The overall modeling period, 1961–2020, was divided into decades (1961–1970, 1971–1980, etc.) since these intervals correspond to key stages of environmental transformation and represent the conventional time framework for ecological and geographical studies of the Aral Sea crisis. Decades are numbered chronologically as follows:  $N = 1$  for 1961–1970,  $N = 2$  for 1971–1980, and so forth.

In [10], assuming that vegetation degradation depends on both the deterioration of the regional water regime and the impact of salt transport, by comparing data series on vegetation changes, Amu Darya discharge in the lower reaches, and calculated dry deposition rates, and by approximating the results of numerical modeling, the following relationship was obtained:

$$D_f(x, y, t) = 0,01t \left[ 49 \exp(-W_r) + 0,8 \frac{C_N}{C_{cr}} \right] \quad (1)$$

Where  $C_{cr}$  – the critical level of dry salt deposition at which destructive effects on plants begin (34 kg/ha [6, 7, 8]);

$C_N$  – the dry deposition of saline aerosol, calculated as

$C_N = 3,3kV \exp(-0,015x - 0,6)$ ,  $Wr = 1,307 \exp(-0,0619 t)$  – the ratio of Amu Darya discharge in a given year to that of 1961.

If the projected vegetation cover in a given location at the initial year (1961) is denoted by  $\delta_0$ , then obviously

$$\delta_f(x, y, t) = \delta_f(x, y, 0) [1 - 0,01D_f(x, y, t)] \quad (2)$$

Since this study focuses solely on the salt factor, i.e., the influence of salt transport (ST), the  $Wr$  term in Equation (1) is omitted. Moreover, it is necessary to account for the salinization of soils in the Southern Aral region by salt aerosols from the Aralkum, which occurs due to the vertical infiltration of dry aerosol depositions into the soil and their subsequent leaching by precipitation [10]:

$$\Delta S_s = 0,45C_N + 0,47M_{dep} - 20,73 \quad (3)$$

Where  $CN(x, z, t)$  represents dry deposition and  $M_{dep}$  is the mineralization of liquid precipitation, calculated as

$$M_{dep} = \frac{1}{R + \Delta R} \int C(x, z, t) dz, \quad \Delta R = -1,5E-5C^3 + 6,1E-4C^2 + 0,189C + 1,81 \quad (4)$$

$C(x, z, t) = 3,3kV(t) \exp(-0,015x - 0,3z - 0,6)$  where  $C$  is the atmospheric salt concentration.

The dependence of total projected cover (TPC) reduction on  $\Delta S_s$  is derived from the known relationship between TPC and soil salinity [5]:

$$\Delta \delta_s = k \Delta S_s \quad (5)$$

Finally, vegetation degradation under the influence of salt transport from the dried Aral Sea bed (DASB) at a given point  $(x, y)$  and time  $t$  can be expressed as:

$$D_f(x, y, t) = 0,01t \left[ \Delta S_s + 0,8 \frac{C_N}{C_{cr}} \right] \quad (6)$$

The salt deposition field  $C_N$  was computed separately for each wind direction using the formula obtained in [10] by approximating the results of long-term numerical modeling of the salt transport process from the DASB:





$$C_N(i, N) = 3,3kV(N) \exp(-0,015x - 0,6)f_i(N) \quad (7)$$

Where  $V(N) = Ptr(N)$   $Ssal(N)$  – the annual volume of salt transport from the entire DASB;  $Ptr$  – the potential of salt transport [10];

$Ssal(N)$  – the area of saline surfaces;

$x$  – the distance from the source of salt transport (km);

$f_i(N)$  – the frequency of the  $i$ -th wind direction during the  $N$ -th decade.

The dynamics of the salt transport potential (STP) are described by a linear relationship:

$Ptr(N) = -311N + 7685$ , and the dynamics of saline surface area by:

$$S_{sal}(N) = 0,0042 (S_s)^2 + 0,073 S_s \quad [10].$$

The areal source of salt transport (the Aralkum Desert) was approximated by a set of point sources (salt flats), which adequately reflects the real conditions. The total annual salt transport  $V(N)$  from the entire Aralkum equals the sum of emissions from each point source  $V_k(N)$ . The deposition field  $CN$  for each source was calculated in a polar coordinate system, with the angle  $\varphi$  covering eight prevailing wind directions. The resulting field  $CN$  from the  $k$ -th source was then projected onto a global Cartesian coordinate system (OXY):

$$CN(\rho, \varphi) \rightarrow CN(X, Y) \rightarrow CN(\rho, \varphi) \rightarrow CN(X, Y)$$

The origin of the coordinate system was aligned with the lower-left corner of the modeled area, with the  $OX$  axis directed along the southern boundary and the  $OY$  axis along the western boundary (Fig. 2).

The surface concentration field from all sources is evidently the sum of individual contributions:  $\sum [CN(X, Y)]k$ .

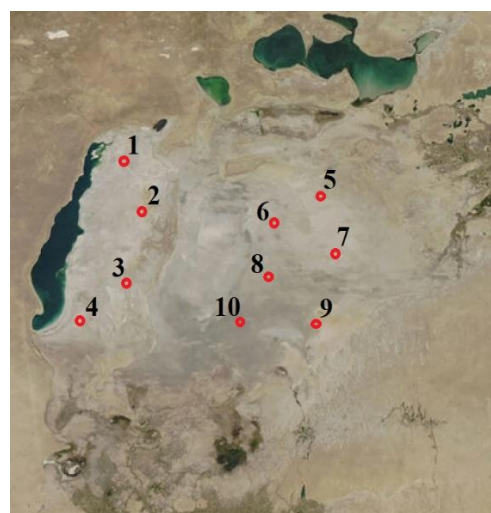


**Figure 2.** Main sources of salt transport

Using Equation (6), which describes the degree of vegetation damage by saline aerosol, we obtained the spatial dynamics of vegetation cover under the influence of salt emissions from the dried Aral Sea bed (DASB) for each  $N$ -th decade.

## Data

The primary sources of information include a limited number of publications on this topic, satellite imagery, electronic databases, meteorological archives on wind regimes, and the results of our own field experiments [9]. To process both empirical and modeled data, we employed spatio-



temporal interpolation, correlation analysis, factor analysis, and GIS technologies.

Meteorological parameters were averaged for the vegetation period. The data indicate a trend toward increasing wind speed, while the amount of precipitation has decreased during the 2000–2020 period [18]. Thus, the dynamics of meteorological parameters contribute to the intensification of salt transport (ST).

The wind direction over the Aralkum Desert varies from year to year. Variations in the direction of salt transport are caused by changes in the general atmospheric circulation (GAC) associated with the alternation of circulation epochs [7] and the effects of global warming. Overall, the data show that approximately **70% of salt transport occurs toward the west–south sector**, i.e., in the direction of the territory of Karakalpakstan (Fig. 3).

Figure 3. Predominant wind directions and main paths of salt transport from the Aralkum

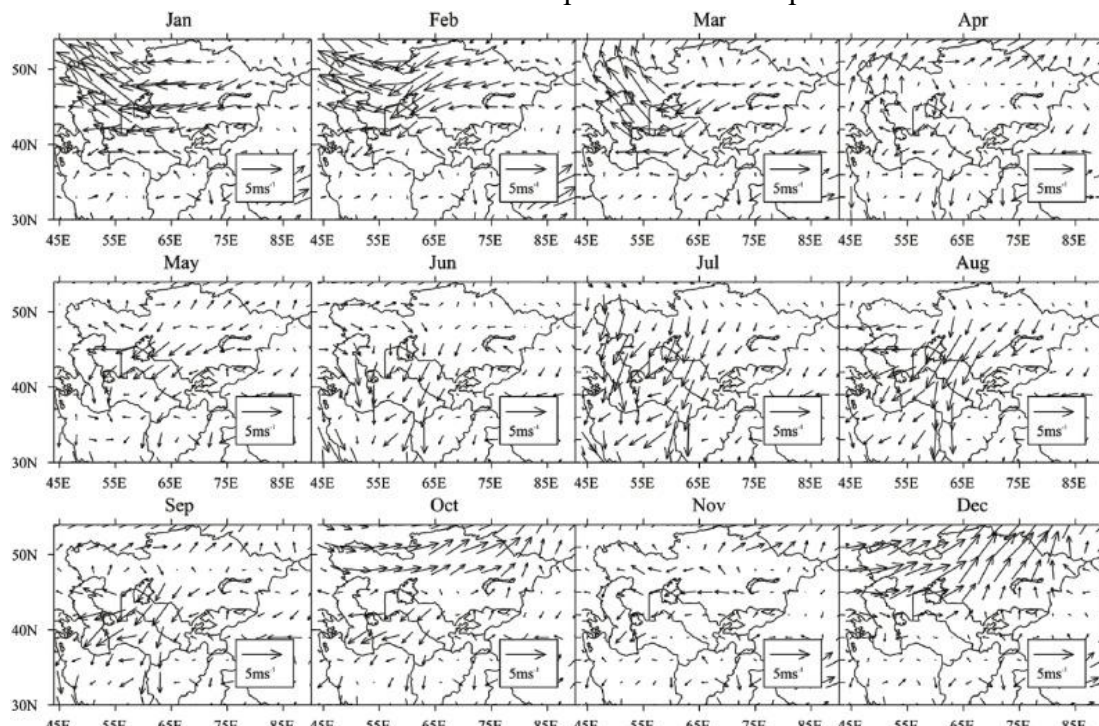


**Fig. 3. Annual pattern of the wind field at the 1000 hPa level (averaged from 1980 to 2018 using ECMWF datasets).**

The character of the wind and the difference between the 850 hPa and 1000 hPa levels determine the direction and intensity of aerosol transport in the atmosphere. The vertical wind shear between 1000 and 850 hPa causes intrusions of cold air from the north, northwest, and northeast directions [18]. However, wind vectors at the 1000 hPa level can reliably be used to represent the surface wind field [16].

Grigoriev and Lipatov [3], based on an analysis of satellite images from 1975–1981, identified three main directions of dust plume flows. In 60% of cases, dust storms were directed southwestward, in 25% — westward, and the remaining 15% — southward and southeastward.

More recent studies [15,18] indicate the following directions of salt transport from the dried-up Aral Sea bottom (Fig. 4).



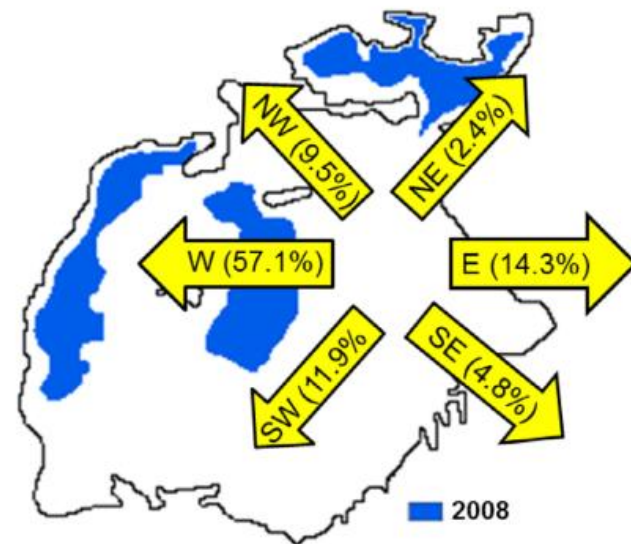


**Fig. 4. Directions of dust storm plumes during 2005–2008 [15].**

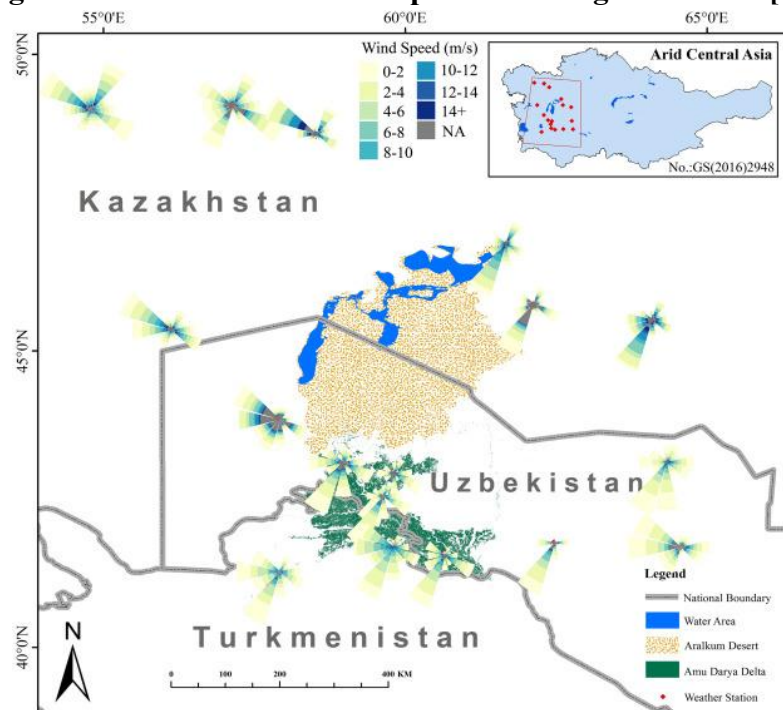


**Fig. 5. Directions of dust storms for 17 meteorological stations in the Aral Sea region, averaged for 2005–2020 [18].**

In Uzbekistan, Kazakhstan, and Turkmenistan, a long-term dust deposition monitoring program covering 21 stations showed that during 2003–2010, the aeolian transport of dust occurred mainly in the southern direction [13] (Fig. 6).

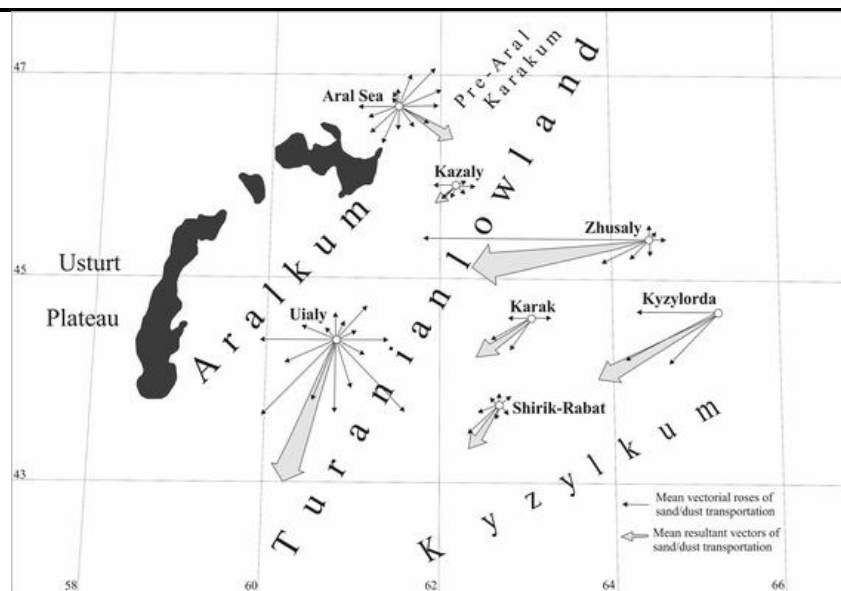


**Fig. 6. Directions of sand and dust transport in the Aral Sea region.**

A detailed statistical analysis of data from the Muynak meteorological station [11], which served as the basis for our calculations, shows a significant predominance of winds from the northern half of the compass throughout the entire modeling period (Fig. 7).

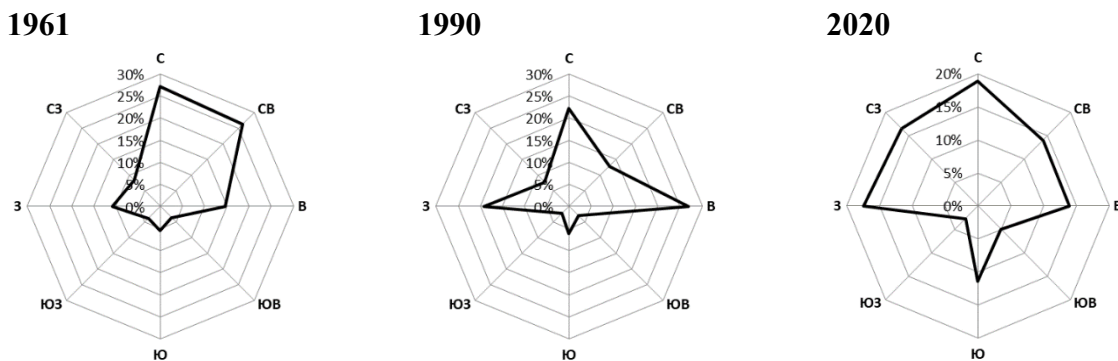


**Fig. 7. Spatio-temporal dynamics of the annual wind rose (Muynak meteorological station).**

As a result of field experiments conducted in 2022–2024 [9], preliminary calculations of the maximum permissible concentrations (MPC) of salts from the dried Aral Sea bottom (mainly sodium and potassium sulfates,  $\text{Na}_2\text{SO}_4$  and  $\text{K}_2\text{SO}_4$ ) were obtained for several typical communities of wild-growing plants. Long-term exposure to average ten-day dry salt depositions of  $\text{Na}_2\text{SO}_4$  at levels of 5, 10, 15, and 20  $\text{g}/\text{m}^2$  leads to a decrease in total projective vegetation cover by the end of the growing season (for *Climacoptera brachiata*, *Glycyrrhiza glabra*, *Climacoptera aralensis*) by an average of 10%, 17%, 25%, and 30%, respectively.

Single dust storm exposure results in plant mortality (*Aeluropus litoralis*, *Daucus acutiloba*) at dust concentrations of  $20 \text{ mg}/\text{m}^3$  under unfavorable conditions (dust storms with precipitation) and at concentrations exceeding  $50 \text{ mg}/\text{m}^3$  under normal conditions (*Artemisia terrae-albae*, *Artemisia turanica*, *Halimodendron holodendron*).





The obtained data were used to determine **Ccr** — the critical value of dry salt deposition (34 kg/ha), at which destructive effects on vegetation begin.

## Results

The calculated fields of **CN**, the mean annual value of dry salt deposition, for example, for 1990 and 2024, are shown in Figs. 8 and 9. The highest amounts of dry salt deposition in both years are observed in the Kungrad and Muynak districts, i.e., the territories located to the southwest of the Aralkum Desert. This indicates the stability of the prevailing direction of salt transport from the desiccated sea bottom.

By comparing Figs. 7 and 8, one can note how much the area affected by salt transport from the Aralkum has expanded. In 1990, the 20 kg/ha dry deposition isoline extended about 150 km south and 500 km southwest of the Aralkum, whereas in 2024 this isoline reaches 300 km south and 800 km southwest.

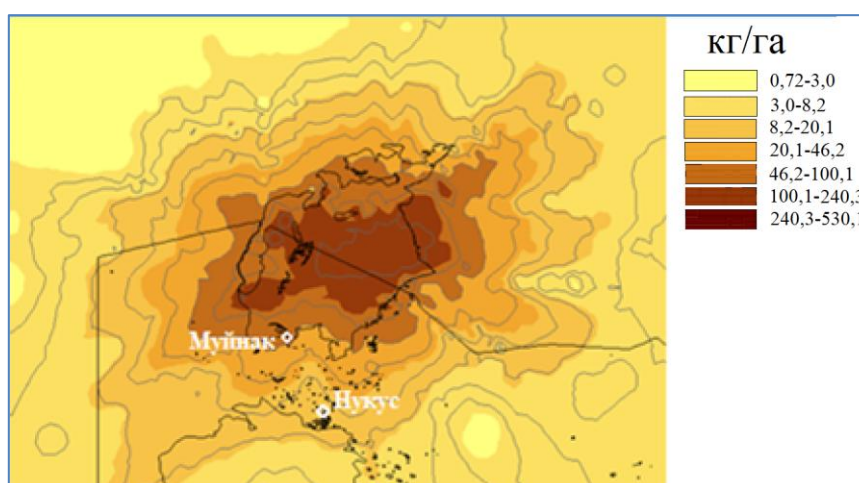


Fig. 8. Average annual dry salt deposition in 1990 (kg/ha)

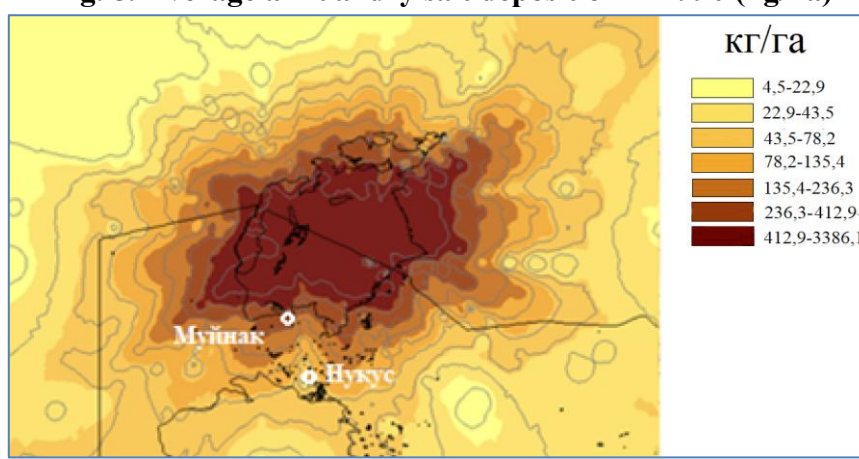


Fig. 9. Average annual dry salt deposition in 2024 (kg/ha)

The corresponding fields of reduction in the total projective cover (TPC) of vegetation communities are shown in Figs. 10 and 11. The zone of significant stress (more than 0.4% annual decrease in TPC) occupied an area of 4.6 km<sup>2</sup> in 1990 and 20.1 km<sup>2</sup> in 2024.



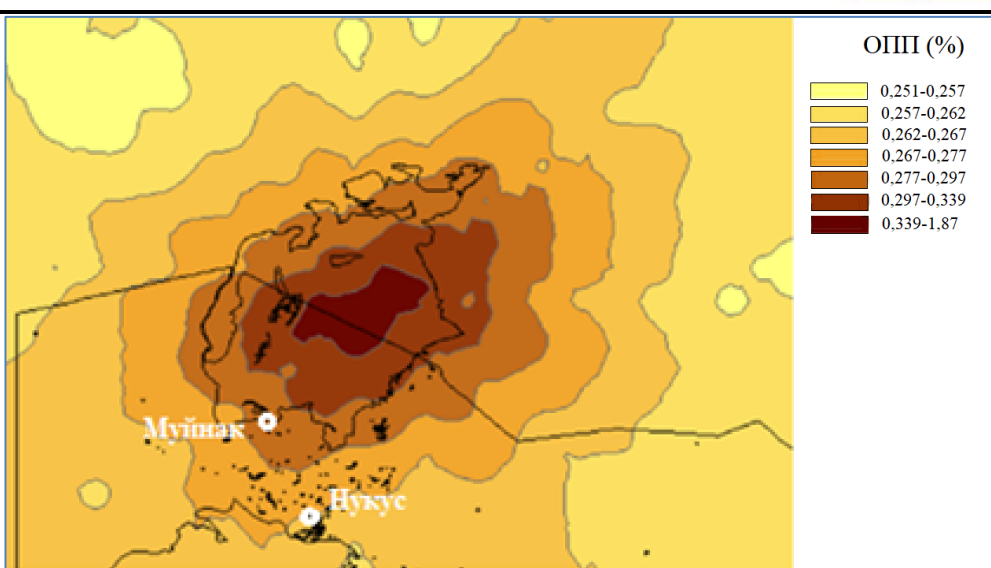


Fig. 10. Reduction of vegetation TPC under the influence of dry salt deposition in 1990 (%)

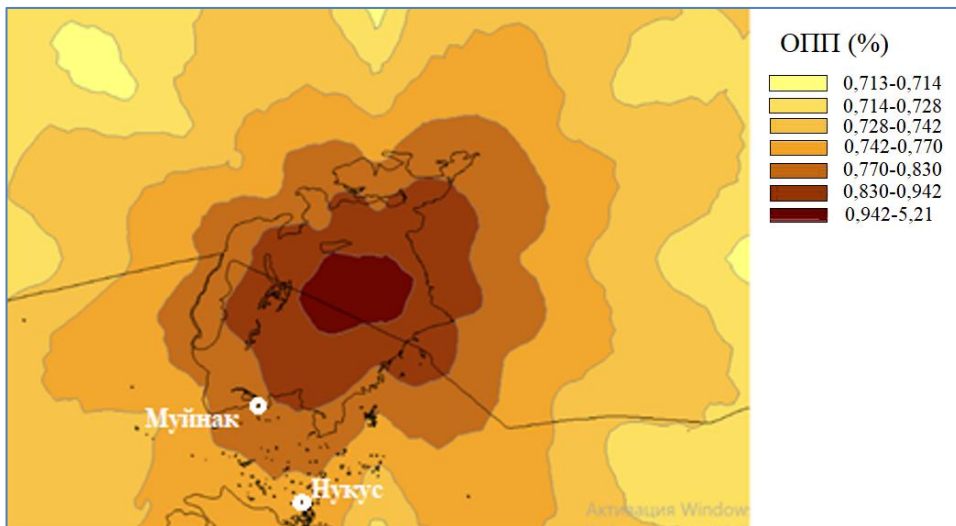


Fig. 11. Reduction of vegetation TPC under the influence of dry salt deposition in 2024 (%)

Based on the results of long-term modeling of the spatio-temporal dynamics of vegetation degradation in the Southern Aral Sea region, a generalized formalized expression of this dynamic was obtained for the entire region (Figs. 12 and 13).

The dynamics of TPC reduction, both on the Ustyurt Plateau and in the lower reaches of the Amu Darya River, follows a logarithmic law. The initially high rates of TPC decline observed during the first decade under the influence of salt storms gradually slowdown in subsequent decades due to ecological succession accompanied by an increasing proportion of halophytic species in plant communities, as well as the adaptive capacity of vegetation.



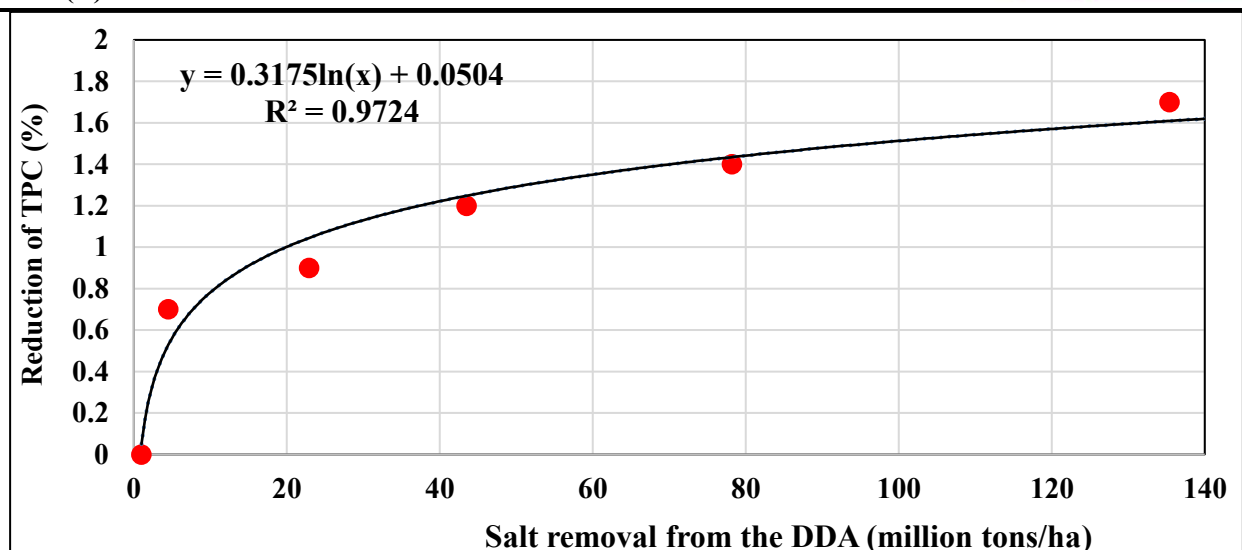


Fig. 12. Influence of salt transport (dry deposition) on the Ustyurt Plateau

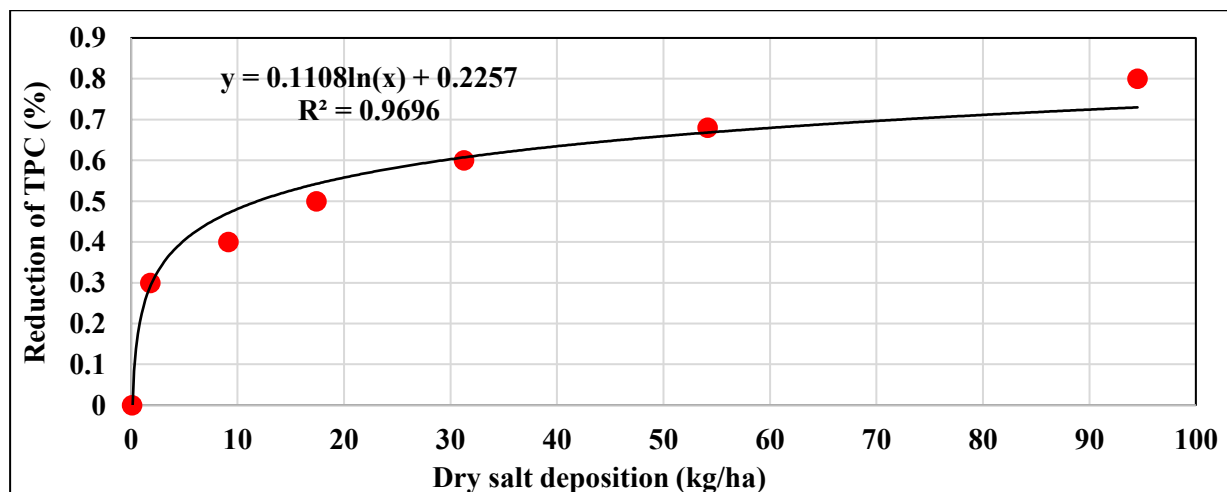


Fig. 13. Influence of salt transport (dry deposition) in the lower reaches of the Amu Darya River

Verification of the modeling results was carried out using available actual data on the total projective cover (TPC). Spatial comparison (area-based) between modeled and observed data was performed by processing satellite images with the *LpSquare* software.

### Conclusion

This study provides a quantitative assessment of the impact of salt transport from the Aralkum Desert on the total projective cover (TPC) of vegetation. Accordingly, only one aspect of vegetation evolution was considered — the reduction in vegetation-covered areas. The effect of the salt factor increases significantly when considering successional and physiological destructive processes caused by salts from the Aralkum. Based on the research results, the following conclusions were drawn:



1. The reduction of TPC under the influence of salt storms (SS) is progressing at an average rate of 0.4% per year. While in 1990 the average seasonal decrease across the region (including Aralkum) was 1.4%, by 2024 this figure had risen to 18.3% per year.
2. The strongest effect of SS occurs in Kungirot and Muynak districts, where the reduction of vegetation cover during the growing season in 2024 reached 9.1% and 13.7%, respectively.
3. Summing the annual reductions in TPC over the entire Aral crisis period gives an impressive total degradation of vegetation cover across the region — from 20% to 50%.
4. The assessment of the dependence of the process on any single factor is complicated due to the interactions between the process itself and environmental elements. In field studies of SS impact on vegetation, meteorological conditions (wind, precipitation) play a major role. To eliminate their influence, laboratory experiments in controlled environments are required.
5. Field experiments should be continued and refined due to remaining uncertainties — including threshold concentrations differentiated by plant species, individual contributions of various impact mechanisms, influence of local soil conditions (mechanical and mineral composition), and meteorological variability.
6. Considering the 10–20% decline in plant biomass and productivity under the influence of sulfates from the dried Aral seabed, it is urgent to expand research in this area and intensify efforts to reduce salt and dust emissions from the Aralkum, including artificial precipitation techniques.

## References

1. Allanazarov, K. Zh., & Satbaev, T. (2005). Climatic conditions, agro-climatic resources of the Amu Darya delta, and their changes due to desertification. In **Proceedings of the Scientific-Practical Conference “Study of Environmental Problems of the Aral Sea Region”** (pp. 1–2). Nukus, Uzbekistan.
2. The Aral Sea and the Aral Region. (2015). Retrieved from <http://www.cawaterinfo.net/library/rus/watlib/watlib-16-2015.pdf>
3. Grigoriev, A. A., & Lipatov, V. B. (1985). Dust storms according to space research data. Leningrad: Gidrometeoizdat.
4. Dukhovny, V. A., Razakov, R. M., Ruziyev, I. B., & Kosnazarov, K. K. (1984). Problems of the Aral Sea and environmental protection measures. Problems of Desert Development, (6), 3–15.
5. Kublanov, Zh. Zh., & Tleumuratova, B. S. (2022). Some aspects of the development of phytocenoses on the dried bottom of the Aral Sea. Bulletin of the Karakalpak Branch of the Academy of Sciences of the Republic of Uzbekistan, (3), 69–75.
6. Safarov, A. (2005). Influence of soil salinity on the development and productivity of amaranth. In **Proceedings of the Scientific-Practical Conference “Study of Environmental Problems of the Aral Sea Region”** (pp. 1–2). Nukus, Uzbekistan.
7. Subbotina, O. I., & Chanyshева, S. G. (2006). Climate of the Aral Sea Region. Tashkent: NIGMI.
8. Tazhimuratov, P., Pirzhanova, R., & Seitniyazova, B. (2005). Changes in the phytocenosis of the coastal zone of Ustyurt under aridization. In **Proceedings of the Republican Conference “Study of Environmental Problems of the Aral Sea Region.”** Nukus: Bilim, 3–4.





9. Tleumuratova, B. S., Kublanov, Zh. Zh., & Urumbaev, A. E. (2024). Pollution of vegetation cover by sulfates from the dried bottom of the Aral Sea. *Bulletin of the Karakalpak Branch of the Academy of Sciences of the Republic of Uzbekistan*, (1), 54–60.
10. Tleumuratova, B. S. (2018). Mathematical modeling of the influence of ecosystem transformations of the Southern Aral Sea region on soil-climatic conditions. Doctoral dissertation (D.Sc. in Physical and Mathematical Sciences), Tashkent, 209 p.
11. Urazymbetova, E. P. (2024). Modeling of atmospheric dust pollution in Karakalpakstan from the Kyzylkum Desert. *Economics and Society*, 4-1(119), 1126–1131.
12. Southern Aral Sea Region – New Perspectives. (2003). Edited by Prof. V. A. Dukhovny & Eng. J. De Schutter. Tashkent, p. 156.
13. Groll, M., et al. (2003). Aeolian dust deposition in the Aral Sea region – A spatial and temporal analysis of an ecological crisis.
14. The Great Green Wall: A Project of Hope for the African Continent. (2023, August 14). Retrieved from <https://ecosphere.press/2023/08/14/velikaya-zelenaya-stena-proekt-nadezhda-afrikanskogo-kontinenta/>
15. Indoitu, R., Kozhoridze, G., Batyrbaeva, M., Vitkovskaya, I., Orlovsky, N., Blumberg, D., & Orlovsky, L. (2015). Dust emission and environmental changes in the dried bottom of the Aral Sea. *Aeolian Research*, 101–115.
16. Shi, L., Zhang, J., Yao, F., Zhang, D., & Guo, H. (2020). Temporal variation of dust emissions in dust sources over Central Asia in recent decades and the climate linkages. *Atmospheric Environment*, 222, 117176.
17. Novikova, N. M. (1998). Contemporary plant and soil cover changes in the Amudarya and Syrdarya river deltas. In **Ecological Research and Monitoring of the Aral Sea** (pp. 100–128). UNESCO.
18. Wang, W., Samat, A., Abuduwaili, J., Ge, Y., De Maeyer, P., & Van de Voorde, T. (2022). Temporal characterization of sand and dust storm activity and its climatic and terrestrial drivers in the Aral Sea region. *Atmospheric Research*, 275, 106242. <https://doi.org/10.1016/j.atmosres.2022.106242>

